

# What Moves You: Using Legs for Vehicular Transportation

Jonathan Graf<sup>1</sup>  
Olga Stulov<sup>2</sup>  
Sponsor: James Sochacki<sup>3</sup>

**Abstract.** Most vehicles are transported by the rotation of wheels. The Department of Mathematics and Statistics and Department of Engineering at James Madison University are interested in developing vehicles that will be driven by the motion of legs rather than wheels. In this paper we discuss the motion of five different legs: first, we derive the equations of motion for each leg; second, we calculate the equations for velocity, acceleration, energy and power; third, we optimize the motion by minimizing energies and forces. In order to obtain these results, we developed a differential equation, solved it using the Parker-Sochacki Method and reached the optimal solution using Maple's minimization package.

## 1 Introduction

Most vehicles are transported by the rotation of wheels. Existing wheeled vehicles can only access less than half of the Earth's landmass. Meanwhile, animals and people can go almost anywhere simply using their legs.

For this reason Boston Dynamics developed a rough-terrain robot called BigDog that carries heavy loads while walking, running, and climbing. By traveling 12.8 miles without a stop to refuel, BigDog holds a world's record for legged vehicles. It carries 340 lbs, runs at 4 mph, climbs hiking trails of up to 35 degree slopes, and walks in water and snow. The pictures below are the images of BigDog [7].



Figure 1: BigDog In Action

The James Madison University (JMU) Engineering Department is interested in developing its own vehicles that will be driven by the motion of legs rather than wheels. Determining the motion of these legs is an interesting research problem because of all the moving parts of a leg. In this report we will focus on mathematically modeling the motion of two types of legs for different transportation uses [6].

We provide a picture of the schematic of a robot leg and a computer generated image of an optimized modification of this leg (Figure 2). We will present the mathematical model of the original

<sup>1</sup>jonathansgraf@gmail.com, Towson University

<sup>2</sup>olga.stulov@gmail.com, State University of New York at New Paltz

<sup>3</sup>jim@math.jmu.edu, James Madison University, Department of Mathematics and Statistics

robot leg and the process we used to obtain the computerized robot leg. The red pivots in Figure 2 are fixed points of the legs. Therefore, the segments connected to them trace out a portion of a disk. The remaining points move during the motion of the legs. The two curves on the computerized leg represent the motion of the ‘foot’ and ‘knee’ as the leg moves.

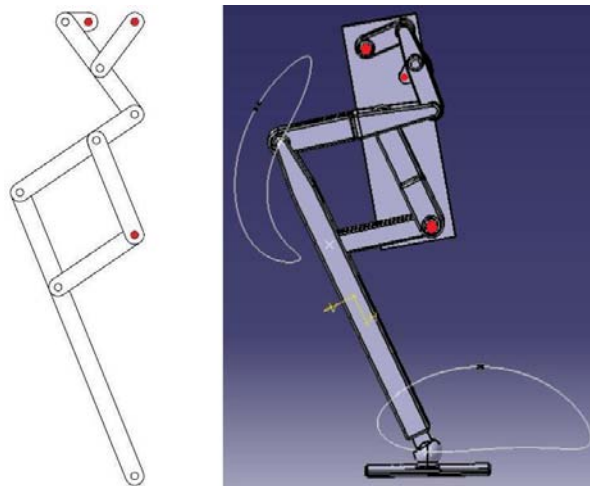


Figure 2: Schematic (left) and Computerized (right) of Two Robot Leg Images

The outline of our paper will be as follows. We present an analysis of five different transportation legs. In Section 2 we introduce the five legs, the transportation use of the leg and the parametric equations for the motion of the legs. In this section we start by showing simple legs (Sections 2.1 and 2.2) that lead to the construction of the more complex legs such as the ones displayed in Figure 2. In Section 3 we give the velocities and accelerations of the critical points for the motion of the legs. Finally, in Section 4 we use the results of Sections 2 and 3 to present our optimized legs. We conclude with a summary of our results and a discussion of future research.

## 2 Leg Systems

We worked with Roger Thelwell [9], a professor in the Department of Mathematics at JMU, Florian Otto [3] and Stefan Trumm [10], engineering students at Hochschule für Technik und Wirtschaft des Saarlandes - University of Applied Sciences in Germany, to develop five legs. The basic idea was to develop a four to six legged robot that would move using these legs. In this paper we present the legs and mathematically analyze the legs for optimal engineering design. The design of the robot is future work.

We only consider the motion of the leg in a vertical plane. The horizontal axis in the plane will be the  $x$ -axis. The vertical axis in the plane will be the  $y$ -axis. Therefore, subscripts  $x$  and  $y$  will be used to denote the coordinates of points and components of vectors in the horizontal and vertical directions, respectively, in this plane. A rotating pivot attached to a line segment will drive all legs. This line segment will trace out a portion of a disk.

### 2.1 Thelwell Leg

The first design of the leg that we worked with is shown in Figure 3 and is called the Thelwell Leg. The four components of the leg are connected by the points labeled in Figure 3 where

- point O is a fixed point, which for simplicity we set as the origin of our 2D coordinate system
- point C is a fixed point of the leg that is to model a ‘hip’
- point P moves
- point Q is the driving point of the system tracing out a circle of radius OQ. It is driven by pivot O rotating at a fixed speed and moves the ‘foot’
- point R is the ‘foot’ of the system.

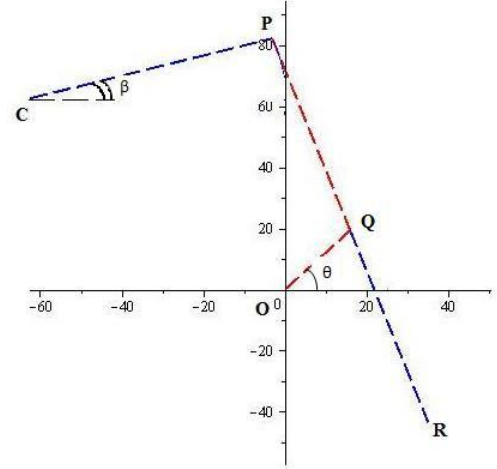


Figure 3: Thelwell Leg

The lengths of all four segments (CP, PQ, OQ, QR) are fixed. We will denote components of the leg as follows:

- $r_{OQ}$  is constant and the radius of the circle traced out by Q
- $r_{CP}$  is constant and the radius of a partial circle traced out by P
- $l_{PQ}$  is the length of PQ and constant
- $l_{QR}$  is the length of QR and constant
- $k_{PR} = \frac{l_{PQ} + l_{QR}}{l_{PQ}}$  is a length ratio used to simplify notation later.

In order to parametrize the motion of points P, Q and R we use the angles  $\theta$  and  $\beta$  in Figure 3. We use  $t$  as the parameter. Therefore,

- $\theta(t)$  - the angle between the positive  $x$ -axis and the radius OQ and is given
- $\beta(t)$  - the angle between the positive  $x$ -axis and the radius CP and is determined by  $\theta(t)$ .

The  $x$  and  $y$  coordinates of the points in terms of these two angles and the origin are given in Table 1.<sup>4</sup>

Point	$x$ coordinate	$y$ coordinate
O	0	0
C	$x_0 = -r_{CP}$	$y_0 = l_{PQ}$
P	$C_x + r_{CP} \cos(\beta(t))$	$C_y + r_{CP} \sin(\beta(t))$
Q	$r_{OQ} \cos(\theta(t))$	$r_{OQ} \sin(\theta(t))$
R	$P_x + k_{PR}(Q_x - P_x)$	$P_y + k_{PR}(Q_y - P_y)$

Table 1: The Coordinates of the Thelwell Leg

We assume the angle  $\theta$  is given by

$$\theta(t) = \frac{vt}{r_{OQ}},$$

where  $v$  is a given constant speed of the driving point Q, moving around the circle centered at O, and  $t$  is the unit of time.

<sup>4</sup>Note:  $C_x$  and  $C_y$  are the  $x$  and  $y$  coordinates of point C, respectively. The similar notation is applied to the rest of the points as well.

### Solving for angle $\beta$ :

Since PQ is a fixed length, we first solve for  $\beta_0 = \beta(0)$ . Using the Pythagorean Theorem

$$(C_x + r_{CP} \cos(\beta_0) - r_{OQ})^2 + (C_y + r_{CP} \sin(\beta_0))^2 = (l_{PQ})^2.$$

This quadratic equation generates two solutions for  $\beta_0$ . We select from these the physically correct value by taking the value between  $-\frac{\pi}{2}$  and  $\frac{\pi}{2}$  as this satisfies the physical constraint of the leg system.

Since for all  $t$ ,  $\beta$  solves this equation, we had to develop a method to obtain the physically correct solution for  $\beta(t)$ . To do this, we differentiated this equation with  $\beta_0$  replaced by  $\beta(t)$ . Ordinary differential equations (ODEs) of our form have a unique solution [1] as will be outlined later. Therefore,  $\beta(t)$  is determined by the correct  $\beta_0$  from this differential equation. We used Maple to derive the IV ODE as

$$\frac{d\beta(t)}{dt} = \frac{r_{OQ} \left( \frac{d\theta(t)}{dt} \right) (C_x \sin(\theta(t)) + r_{CP} \cos(\beta(t)) \sin(\theta(t))) - C_y \cos(\theta(t)) - r_{CP} \sin(\beta(t)) \cos(\theta(t))}{r_{CP} (C_x \sin(\beta(t)) - r_{OQ} \cos(\theta(t)) \sin(\beta(t)) - \cos(\beta(t)) C_y + \cos(\beta(t)) \sin(\theta(t)) r_{OQ})}.$$

This IV ODE is best solved numerically. To do so we apply the Parker-Sochacki Method (PSM) [4]. The PSM is a modified Picard Iteration algorithm used to solve systems of IV ODEs. The PSM produces the numerical solution as piecewise Maclaurin polynomials to a chosen degree over a chosen time step (interval). The coefficients in the Maclaurin polynomial can be either algebraic or numeric. We demonstrate the PSM implementation step by step for our IV ODE.<sup>5</sup>

The first step is to convert the IV ODE to an equivalent polynomial system of IV ODEs by making auxiliary substitutions. In our case, we make the following eight substitutions

$$\begin{aligned} y_1 &= \beta(t) \\ y_2 &= \sin(\beta(t)) \\ y_3 &= \cos(\beta(t)) \\ y_4 &= \frac{1}{y_8} \\ y_5 &= \sin(\theta(t)) \\ y_6 &= \cos(\theta(t)) \\ y_7 &= \theta(t) \\ y_8 &= r_{CP}[C_x \sin(\beta(t)) - r_{OQ} \cos(\theta(t)) \sin(\beta(t)) - C_y \cos(\beta(t)) + r_{OQ} \sin(\theta(t)) \cos(\beta(t))]. \end{aligned}$$

Technically, we could have done only seven substitutions putting the fourth and eighth equations together. However, using our eight substitutions gives a system that is less computationally intensive.

The second step is to take the derivative of each substitution with respect to time

$$\begin{aligned} y_1' &= \beta'(t) = r_{OQ} \cdot y_7' (C_x \cdot y_5 + r_{CP} \cdot y_3 \cdot y_5 - C_y \cdot y_6 - r_{CP} \cdot y_2 \cdot y_6) y_4 \\ y_2' &= y_3 \cdot \beta'(t) = y_3 \cdot y_1' \\ y_3' &= -y_2 \cdot \beta'(t) = -y_2 \cdot y_1' \\ y_4' &= -y_4^2 \cdot y_8' \\ y_5' &= y_6 \cdot \theta'(t) = y_6 \cdot y_7' \\ y_6' &= -y_5 \cdot \theta'(t) = -y_5 \cdot y_7' \\ y_7' &= \theta'(t) \\ y_8' &= r_{CP}[C_x \cdot y_2' - r_{OQ}(y_6' \cdot y_2 + y_6 \cdot y_2') - C_y \cdot y_3' + r_{OQ}(y_5' \cdot y_3 + y_5 \cdot y_3')]. \end{aligned}$$

<sup>5</sup>See [www.math.jmu.edu/~jim/picard.html](http://www.math.jmu.edu/~jim/picard.html) for more papers and codes

In order to use the PSM we have to have initial values. We set the lengths and points in the system to get our initial values as follows:

radius	length	fixed point
$r_{OQ} = 25$	$l_{PQ} = 62.5$	$O(0, 0)$
$r_{CP} = 62.5$	$l_{QR} = 62.5$	$C(-62.5, 62.5)$

Table 2: Physical Constraints of the Thelwell Leg

Finally, we iterate the PSM on this system of IV ODEs to obtain a numerical solution approximated by piecewise Maclaurin polynomials. We use Maclaurin polynomials of degree 8 and a time step  $h = 0.5$ . The piecewise polynomials are generated to approximate  $\beta$  on the interval  $(k - 1)h \leq kh$  for a natural number  $k$ . To cover a sufficient time interval we generate 315 piecewise polynomials that approximate  $\beta(t)$  for  $0 \leq t \leq 315h$  ( $315h$  is approximately  $50\pi$ ). The polynomial generated for the 315<sup>th</sup> iteration for the interval  $314h \leq t \leq 315h$  is

$$\begin{aligned} \beta(t) \approx & 0.37129798733106637539 + 5.7659381392802695795 \cdot 10^{-14} t^8 - 2.1082423172686113233 \cdot 10^{-12} t^7 - \\ & 1.2828032925851222446 \cdot 10^{-10} t^6 + 5.1253133420710030286 \cdot 10^{-10} t^5 + 2.3107023057015958192 \cdot 10^{-7} t^4 \\ & + 0.0000037099059599078413242 t^3 - 0.00047369633525551557248 t^2 - 0.0085763356053177989066 t. \end{aligned}$$

Figure 4 shows a plot of the numerical solution for  $\beta(t)$  for about four periods. Each period of the plot was constructed by continuously connecting the 315 8<sup>th</sup> degree Maclaurin polynomials.

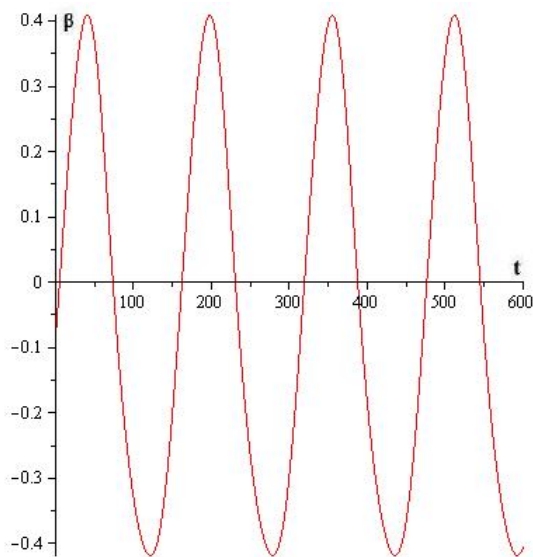


Figure 4:  $\beta(t)$

Since we can now calculate  $\beta(t)$ , from Table 1, we can explicitly find the coordinates for each of the moving points in the leg system (Figure 3). The only possible issue for existence and uniqueness in the IV ODE for  $\beta$  is the denominator defining  $\beta'$  could be zero. However, the geometry of the leg makes this impossible. The geometry of the leg also causes other restrictions. For the fixed point C, we have to be careful with the coordinates. By the Triangle Inequality the coordinates of C must satisfy

$$\|CQ\| \leq \|CP\| + \|PQ\|, \quad \|CR\| \leq \|CP\| + \|PR\|.$$

Parameterizing the four segments of the leg, we have

$$\begin{aligned}
 OQ &= (Q_x \cdot t, Q_y \cdot t) \\
 CP &= (C_x + t(P_x - C_x), C_y + t(P_y - C_y)) \\
 PQ &= (P_x + t(Q_x - P_x), P_y + t(Q_y - P_y)) \\
 QR &= (Q_x + t(R_x - Q_x), Q_y + t(R_y - Q_y)).
 \end{aligned}$$

We display the paths of each point in Figure 5, determined by the parametric equations above, where the blue curve represents the path of point P, the green circle - point Q, and the black curve - point R, respectively, using Maple.

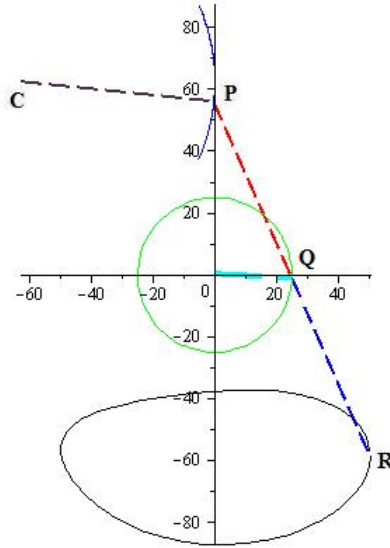


Figure 5: Thelwell Leg and the Paths

This example illustrates how to determine the motion of the Thelwell Leg. The black curve represents the motion of the foot (point R). Next we consider a modification to the leg system above.

## 2.2 Modified Thelwell Leg

The next leg considered was a modification of the Thelwell Leg. The parts of the Thelwell Leg were basically inverted as shown in Figure 6.

Since the modified leg uses the same segments as the Thelwell Leg, we have

- $r_{OQ}$  is constant (the driving wheel of the leg)
- $r_{CP}$  is constant and the radius of a partial circle traced out by P
- $l_{QP}$  is the length of QP and constant
- $l_{PR}$  is the length of PR and constant
- $k_{QR} = \frac{l_{QP} + l_{PR}}{l_{QP}}$  is a length ratio used for simplicity of notation.

To determine the coordinates of this leg's points, we need three angles:  $\theta$ ,  $\alpha$ , and  $\beta$ , all shown in Figure 6. Angle  $\theta$  has the same definition as in the Thelwell Leg, i.e. it is the angle between the positive  $x$ -axis and the radius  $OQ$ . Here  $\alpha$  is the angle between the positive  $x$ -axis and the imaginary line  $QC$ , and  $\beta$  is the angle between the lines  $QC$  and  $PC$ . Recall the following coordinates from the Thelwell Leg

$$\begin{aligned} O_x &= 0 & C_x &= x_0 & Q_x &= r_{OQ} \cos(\theta(t)) \\ O_y &= 0 & C_y &= y_0 & Q_y &= r_{OQ} \sin(\theta(t)) \end{aligned}$$

Using the Pythagorean Theorem, we obtain the length of the line  $QC$  to be

$$l_{QC} = \sqrt{QC_x^2 + QC_y^2},$$

where

$$QC_x = x_0 - r_{OQ} \cos(\theta(t)) ; \quad QC_y = y_0 - r_{OQ} \sin(\theta(t)).$$

Knowing  $QC$  allows us to solve for angle  $\beta$  using the Law of Cosines

$$\cos(\beta(t)) = \frac{(r_{CP})^2 + (l_{QC})^2 - (l_{QP})^2}{2 \cdot l_{QC} \cdot r_{CP}}.$$

To solve for angle  $\alpha$ , we can simply use the slope of the line  $QC$

$$\tan(\alpha(t)) = \frac{y_0 - r_{OQ} \sin(\theta(t))}{x_0 - r_{OQ} \cos(\theta(t))}.$$

As before, using these angles we can write the parametric equations of the coordinates for the rest of the points

$$\begin{aligned} P_x &= x_0 - r_{CP} \cos(\alpha(t) + \beta(t)) \\ P_y &= y_0 - r_{CP} \sin(\alpha(t) + \beta(t)) \\ R_x &= Q_x + k_{QR}(P_x - Q_x) \\ R_y &= Q_y + k_{QR}(P_y - Q_y). \end{aligned}$$

Eventually, having the coordinates of the points allows us to find the equations of the lines using the parametric formulas

$$\begin{aligned} OQ &= (Q_x \cdot t, Q_y \cdot t) \\ CP &= (C_x + t(P_x - C_x), C_y + t(P_y - C_y)) \\ QP &= (Q_x + t(P_x - Q_x), Q_y + t(P_y - Q_y)) \\ PR &= (P_x + t(R_x - P_x), P_y + t(R_y - P_y)). \end{aligned}$$

Putting these equations into Maple with the initial values from Table 3 and setting  $\theta(t) = \frac{13\pi}{10}t$ , we obtain the graph shown in Figure 7 for both the lines and their paths.

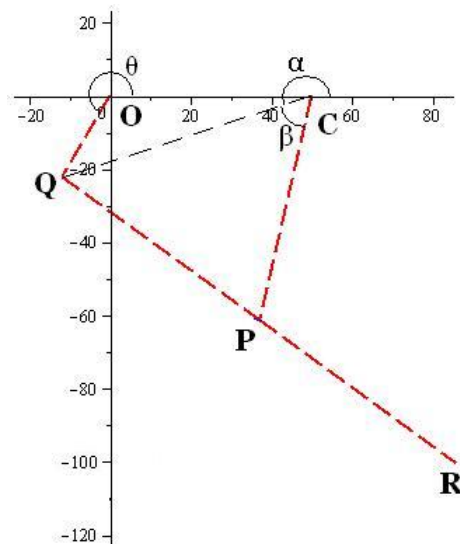


Figure 6: Modified Thelwell Leg



radius	length	fixed point
$r_{OQ} = 25$	$l_{PQ} = 62.5$	$O(0, 0)$
$r_{CP} = 62.5$	$l_{QR} = 62.5$	$C(50, 0)$

Table 3: Physical Constraints of the Modified Thelwell Leg

Modifying the Thelwell Leg in this manner changes the curve drawn by the foot (point R) as can be seen from comparing Figure 7 to Figure 5. Inverting the path of the foot in Figure 7 would give the ‘desired engineer’ path of the foot. Doing this leads to our next leg since the amount of time the foot is on the ground would increase dramatically.

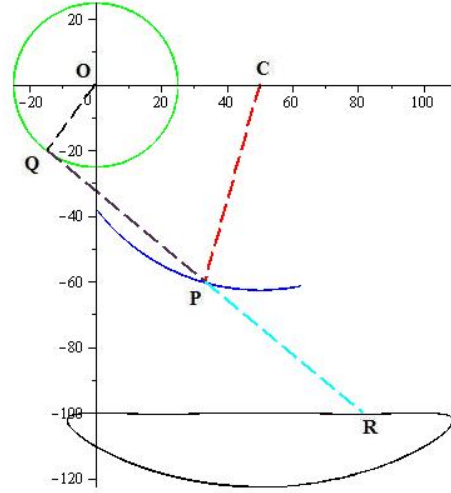


Figure 7: Modified Thelwell Leg with Paths

### 2.3 Otto Leg

Florian Otto [3] was designing a leg for a four-legged human transport vehicle. His desire was to develop a leg with a better path for the foot. That is, a foot that strikes the ground tangentially and remains on the ground for a period of time.

This leg will be more complicated. Basically, a component is added to the Modified Thelwell Leg. This added component will be called the ‘knee’. This knee is the quadrangle FGHI as shown in Figure 8. The point H is the fixed point for the knee.

Observe that the top piece of the Otto Leg (points O, Q, C, P, and R) constitute the Modified Thelwell Leg. Consequently, all the angles, coordinates, and equations for lines of this particular piece are the same as the Modified Thelwell Leg’s. Therefore, we only need to parameterize the points composing the bottom (knee) part. The basic information for the Otto Leg is provided in Table 4.

radius	length		fixed point
$r_{CP} = \text{constant}$	$l_{QP} = \text{constant}$	$l_{GI} = \text{constant}$	$O_x = 0$
	$l_{PR} = \text{constant}$	$l_{IJ} = \text{constant}$	$O_y = 0$
$r_{OQ} = \text{constant}$	$l_{FR} = \text{constant}$	$k_{QR} = \frac{l_{QP} + l_{PR}}{l_{QP}}$	$C_x = x_0$
(the driving wheel of the leg)	$l_{FH} = \text{constant}$	$k_{RG} = \frac{l_{FR} + l_{FG}}{l_{FR}}$	$C_y = y_0$
	$l_{FG} = \text{constant}$	$k_{JG} = \frac{l_{GI} + l_{IJ}}{l_{GI}}$	$H_x = x_1$
	$l_{IH} = \text{constant}$		$H_y = y_1$

Table 4: Otto Leg Data

For angles, we will use  $\theta, \alpha, \beta$ , as previously defined for the Modified Thelwell Leg, and add four new angles for the knee

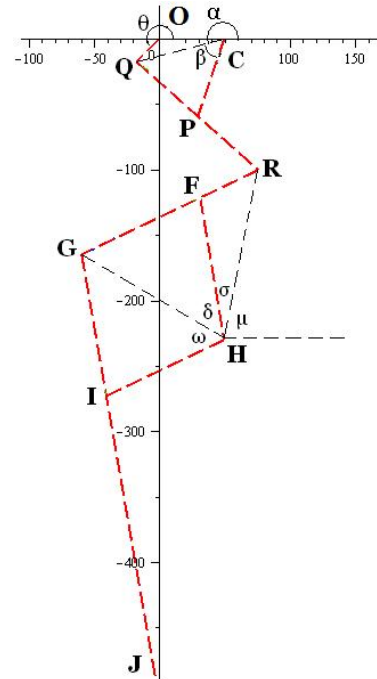


Figure 8: Otto Leg



- $\mu(t)$  - angle between the positive  $x$ -axis and the line  $RH$ <sup>6</sup>
- $\sigma(t)$  - angle between the line  $RH$  and the line  $FH$
- $\delta(t)$  - angle between the line  $FH$  and the line  $GH$
- $\omega(t)$  - angle between the line  $GH$  and the line  $HI$ .

In the case that the quadrangle  $FGHI$  is a parallelogram  $\omega = \delta$ .

To determine the angle  $\sigma$  we use the Pythagorean Theorem and the Law of Cosines, just as we did for angle  $\beta$ . This gives

$$\begin{cases} RH_x = H_x - R_x \\ RH_y = H_y - R_y \end{cases}$$

$$RH = \sqrt{RH_x^2 + RH_y^2}$$

$$\cos(\sigma(t)) = \frac{(l_{FH})^2 + RH^2 - (l_{FR})^2}{2 \cdot RH \cdot l_{FH}}.$$

Angle  $\mu$  can be solved either using tangent or cosine. We choose cosine to generate an angle between 0 and  $\pi$ . Therefore,

$$\cos(\mu(t)) = \frac{R_x - H_x}{RH}.$$

Using angles  $\mu$  and  $\sigma$ , we have that the coordinates of point F are

$$F_x = H_x + l_{FH} \cos(\mu(t) + \sigma(t)) ; F_y = H_y + l_{FH} \sin(\mu(t) + \sigma(t)).$$

Since points R, F, and G are all on the same line, the coordinates of the last point, G, can be derived from the other two points and are

$$G_x = R_x + k_{RG}(F_x - R_x) ; G_y = R_y + k_{RG}(F_y - R_y).$$

Next, the angles  $\delta$  and  $\omega$  can be obtained through the Law of Cosines, since the length of line  $GH$  is

$$GH = \sqrt{(H_x - G_x)^2 + (H_y - G_y)^2}$$

$$\cos(\delta(t)) = \frac{GH^2 + (l_{FH})^2 - (l_{FG})^2}{2 \cdot GH \cdot l_{FH}}$$

$$\cos(\omega(t)) = \frac{GH^2 + (l_{IH})^2 - (l_{GI})^2}{2 \cdot GH \cdot l_{IH}}.$$

From the fixed point H and the four angles  $\mu, \sigma, \delta$ , and  $\omega$ , we derive the coordinates of point I

$$I_x = H_x + l_{IH} \cos(\mu(t) + \sigma(t) + \delta(t) + \omega(t)) ; I_y = H_y + l_{IH} \sin(\mu(t) + \sigma(t) + \delta(t) + \omega(t)).$$

Just as we determined the coordinates of point G through points R and F, we obtain, using G and I, the  $x$  and  $y$  coordinates for point J to be

$$\begin{aligned} J_x &= G_x + k_{JG}(I_x - G_x) \\ J_y &= G_y + k_{JG}(I_y - G_y). \end{aligned}$$

Since we derived the equations of the lines for the top part of the Otto Leg (Modified Thelwell Leg), we only have to parameterize the knee. Figure 9 shows the paths of the points determined by the equations in Table 5 and the initial values given in Table 6.

<sup>6</sup>We are using  $RH$  as the notation here rather than  $l_{RH}$  because this line is not a piece of the leg. Same applies to the line  $GH$ .

line	$x$ coordinate	$y$ coordinate
RF	$R_x + t(F_x - R_x)$	$R_y + t(F_y - R_y)$
FG	$F_x + t(G_x - F_x)$	$F_y + t(G_y - F_y)$
FH	$F_x + t(H_x - F_x)$	$F_y + t(H_y - F_y)$
GI	$G_x + t(I_x - G_x)$	$G_y + t(I_y - G_y)$
IH	$H_x + t(I_x - H_x)$	$H_y + t(I_y - H_y)$
IJ	$I_x + t(J_x - I_x)$	$I_y + t(J_y - I_y)$

Table 5: The Coordinates of the Otto Leg

radius	length		fixed point
$r_{OQ} = 25$	$l_{QP} = 62.5$	$l_{FG} = 100$	$O_x = 0$
$r_{CP} = 62.5$	$l_{PR} = 62.5$	$l_{IH} = 100$	$O_y = 0$
	$l_{FR} = 50$	$l_{GI} = 110$	$C_x = 50$
	$l_{FH} = 110$	$l_{IJ} = 220$	$C_y = 0$
			$H_x = 50$
			$H_y = -230$

Table 6: Physical Constraints of the Otto Leg

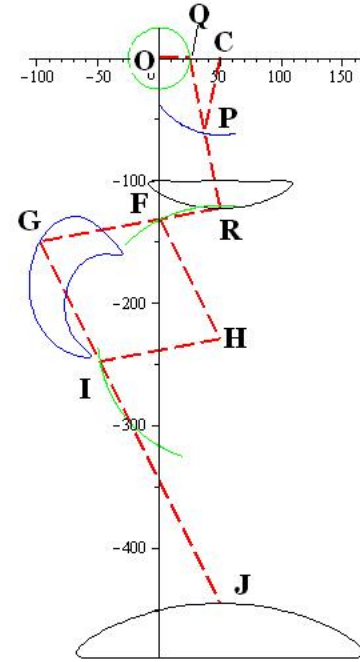


Figure 9: Otto Leg with the Paths

## 2.4 Thelwell Leg and Otto Leg Bottom

An interesting idea is to connect the Otto Leg bottom (knee) to the Thelwell Leg to see how it would influence the curve traced out by the foot. Since all the necessary equations are taken directly from Tables 1 and 5, there is no extra work needed to parameterize this leg. Figure 10 is the diagram of the leg (on the left) and the paths (on the right) for this combination using the initial values in Table 7.

radius	length	fixed point
$r_{OQ} = 20$	$l_{QP} = 31.25$	$O_x = 0$
$r_{CP} = 40$	$l_{QR} = 48.75$	$O_y = 0$
	$l_{FR} = 50$	$C_x = -32.5$
	$l_{FH} = 110$	$C_y = 37.5$
	$l_{FG} = 100$	$H_x = 0$
	$l_{IH} = 100$	$H_y = -140$
	$l_{GI} = 110$	
	$l_{IJ} = 220$	

Table 7: Physical Constraints of the Thelwell/Otto Leg

Comparing the Thelwell bottom curve and the curve generated by the Otto bottom (Figure 10, on the right), one can observe that it traces out the same exact curve, but enlarged and reflected through both the  $x$  and  $y$  axes. This foot hits the ground tangentially and remains on the ground for a short period of time.

In addition, it can be noticed that the curves traced out by the knee and the foot of the Thelwell Leg and Otto Leg Bottom (Figure 10, on the right) are much smoother than the ones of the Otto Leg (Figure 9). Once the prototype of the Otto Leg was built, there was a large amount of torque between certain angles during the rotation of the driving wheel. The sharp edges of the curves

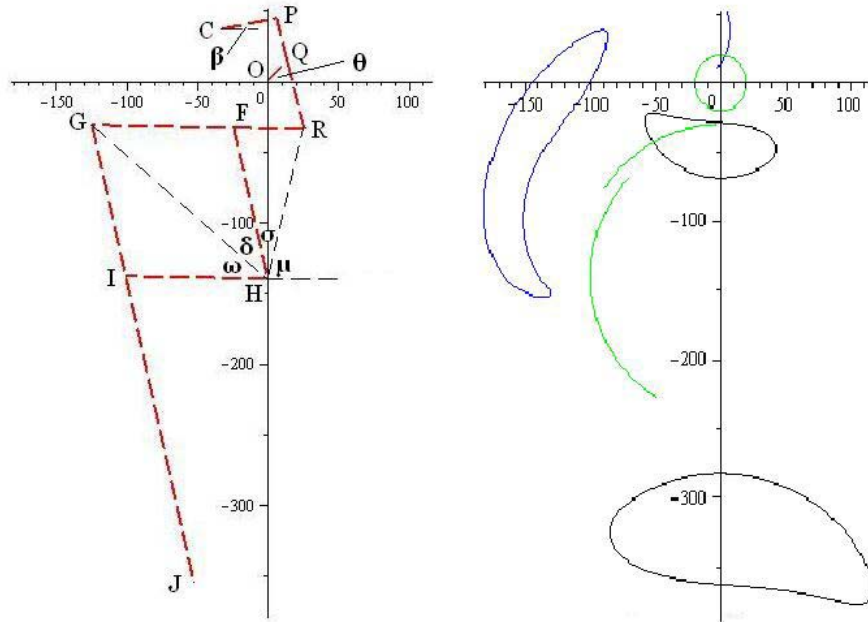


Figure 10: Thelwell/Otto Leg and the Paths

generated by the knee and the foot of the Otto Leg (Figure 9) might indicate the reason for the torque while testing the prototype. This physical flaw was fixed by replacing the top part of the Otto Leg with the Thelwell Leg.

## 2.5 Trumm Leg

Another design that we considered was the Trumm Leg. Trumm’s project was to develop a leg motion vehicle that can transport heavy objects small distances. His design was based on the motion of the legs of the millipede and the kinematic sculptures of Theo Jansen [2]. As in the Otto Leg, the Trumm Leg has a knee (HRST in Figure 11). We note that angles QHR and UST are always right angles independent of the angle  $\theta$  that the driving wheel OP makes with the positive  $x$ -axis.

The Trumm Leg has eight segments and seven pivots (H, O, P, Q, R, S, T). The point U is the foot. We have two fixed points, H and O, where we use O as the origin of the system. As for the angles, we need to determine three angles: one of which was mentioned already ( $\theta$ ), and whose definition stays the same as before; the next angle to be defined is  $\alpha$ , which is the angle between the positive  $x$ -axis and the radius HQ; and the last angle is  $\beta$ , the angle between the positive  $x$ -axis and the length HT.

Thus, the coordinates of point P are

$$P_x = r_{OP} \cos(\theta(t)) ; P_y = r_{OP} \sin(\theta(t)).$$

Since QP is a fixed length, we can solve for  $\alpha_0 = \alpha(0)$  from

$$(H_x + r_{HQ} \cos(\alpha_0) - r_{OP})^2 + (H_y + r_{HQ} \sin(\alpha_0))^2 = (l_{QP})^2.$$

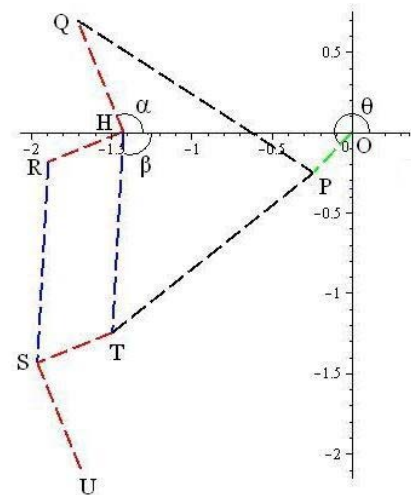


Figure 11: Trumm Leg

Following the same procedure as in the Thelwell Leg when solving  $\beta$ 's ODE, we use  $\alpha_0$  to determine  $\alpha(t)$  from the following IV ODE

$$\frac{d\alpha(t)}{dt} = \frac{r_{OP} \left( \frac{d\theta(t)}{dt} \right) (H_x \sin(\theta(t)) + r_{HQ} \cos(\alpha(t)) \sin(\theta(t))) - H_y \cos(\theta(t)) - r_{HQ} \sin(\alpha(t)) \cos(\theta(t))}{r_{HQ} (H_x \sin(\alpha(t)) - r_{OP} \cos(\theta(t)) \sin(\alpha(t)) - \cos(\alpha(t)) H_y + \cos(\alpha(t)) \sin(\theta(t)) r_{OP})}.$$

As previously, we apply the PSM and make a set of substitutions in the above differential equation

$$\begin{aligned} y_1 &= \alpha(t) \\ y_2 &= \sin(\alpha(t)) \\ y_3 &= \cos(\alpha(t)) \\ y_4 &= \frac{1}{y_8} \\ y_5 &= \sin(\theta(t)) \\ y_6 &= \cos(\theta(t)) \\ y_7 &= \theta(t), \\ y_8 &= r_{HQ} [H_x \sin(\alpha(t)) - r_{OP} \cos(\theta(t)) \sin(\alpha(t)) - H_y \cos(\alpha(t)) + r_{OP} \sin(\theta(t)) \cos(\alpha(t))]. \end{aligned}$$

Then take the derivative of each substitution

$$\begin{aligned} y_1' &= \alpha'(t) = r_{OP} \cdot y_7' (H_x \cdot y_5 + r_{HQ} \cdot y_3 \cdot y_5 - H_y \cdot y_6 - r_{HQ} \cdot y_2 \cdot y_6) y_4 \\ y_2' &= y_3 \cdot \alpha'(t) = y_3 \cdot y_1' \\ y_3' &= -y_2 \cdot \alpha'(t) = -y_2 \cdot y_1' \\ y_4' &= -y_4^2 \cdot y_8' \\ y_5' &= y_6 \cdot \theta'(t) = y_6 \cdot y_7' \\ y_6' &= -y_5 \cdot \theta'(t) = -y_5 \cdot y_7' \\ y_7' &= \theta'(t) \\ y_8' &= r_{HQ} [H_x \cdot y_2' - r_{OP} (y_6' \cdot y_2 + y_6 \cdot y_2') - H_y \cdot y_3' + r_{OP} (y_5' \cdot y_3 + y_5 \cdot y_3')]. \end{aligned}$$

Fixing the lengths and points in the Trumm Leg yields our initial values listed in Table 8. From these we solve for  $\alpha(0)$  and use the PSM.

radius	length	fixed point
$r_{OP} = 0.35$	$l_{QP} = 1.75$	$O_x = 0$
$r_{HQ} = 0.75$	$l_{TP} = 1.6$	$O_y = 0$
	$l_{ST} = 1.5$	$H_x = -1.425$
	$l_{HR} = 1.5$	$H_y = 0$
	$l_{HT} = 1.25$	
	$l_{RS} = 1.25$	

Table 8: Physical Constraints of the Trumm Leg

We again use  $8^{th}$  degree Maclaurin polynomials, but with a time step of 0.0625. To cover a sufficient time interval we generate  $\alpha(t)$  for  $0 \leq t \leq 36h$ . The  $36^{th}$  Maclaurin polynomial generated is

$$\begin{aligned} \alpha(t) \approx & 1.085275580 - 0.7198732220 t^8 + 0.5096067618 t^7 + 0.5325758989 t^6 - 0.1332535767 t^5 - 0.5393973508 t^4 \\ & + 0.5222789003 t^3 + 1.327507812 t^2 - 0.7256833148 t. \end{aligned}$$

The approximate solution for  $\alpha(t)$  for one period is displayed in Figure 12.

We solve for angle  $\beta$  again by deriving  $\beta_0$  through the fixed length TP. The equation for  $\beta_0$  is

$$(H_x + l_{HT} \cos(2\pi - \beta_0) - r_{OP})^2 + (H_y + l_{HT} \sin(2\pi - \beta_0))^2 = (l_{TP})^2,$$

$\beta$ 's IV ODE is

$$\frac{d\beta(t)}{dt} = -\frac{r_{OP} \left( \frac{d\theta(t)}{dt} \right) (H_x \sin(\theta(t)) + \cos(\beta(t)) \sin(\theta(t)) l_{HT}) - H_y \cos(\theta(t)) + l_{HT} \sin(\beta(t)) \cos(\theta(t))}{l_{HT} (-H_x \sin(\beta(t)) - r_{OP} \cos(\theta(t)) \sin(\beta(t)) - \cos(\beta(t)) H_y + \cos(\beta(t)) \sin(\theta(t)) r_{OP}}$$

and its last Maclaurin polynomial is

$$\beta(t) \approx 1.232624953 - 0.1666075280 t^8 + 0.08966140768 t^7 + 0.09750440851 t^6 - 0.1710913627 t^5 - 0.2235884396 t^4 - 0.3003720213 t^3 + 0.7962797792 t^2 + 0.4286716279 t.$$

The approximate solution for  $\beta(t)$  for one period is shown in Figure 13.

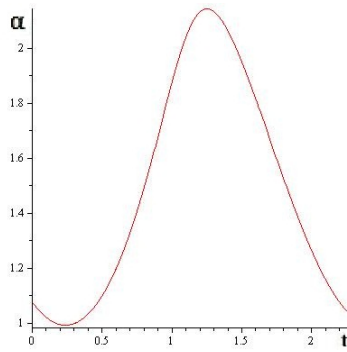


Figure 12:  $\alpha(t)$

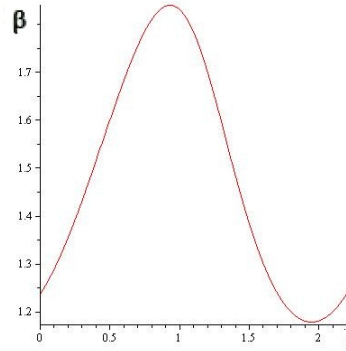


Figure 13:  $\beta(t)$

The angles  $\alpha$  and  $\beta$  allow us to determine the coordinates of points Q, R, and T

$$\begin{aligned} Q_x &= H_x + r_{HQ} \cos(\alpha(t)) & Q_y &= H_y + r_{HQ} \sin(\alpha(t)) \\ R_x &= H_x + l_{HR} \cos\left(\frac{\pi}{2} + \alpha(t)\right) & R_y &= H_y + l_{HR} \sin\left(\frac{\pi}{2} + \alpha(t)\right) \\ T_x &= H_x + l_{HT} \cos(2\pi - \beta(t)) & T_y &= H_y + l_{HT} \sin(2\pi - \beta(t)) \end{aligned}$$

We use a linear transformation to derive the coordinates of the last two points, S and U

$$\begin{aligned} S_x &= R_x + (T_x - H_x) & S_y &= R_y + (T_y - H_y) \\ U_x &= S_x + (H_x - Q_x) & U_y &= S_y + (H_y - Q_y) \end{aligned}$$

Combining all this information, we generate the graph of the Trumm Leg with the paths of the points and show this in Figure 14.

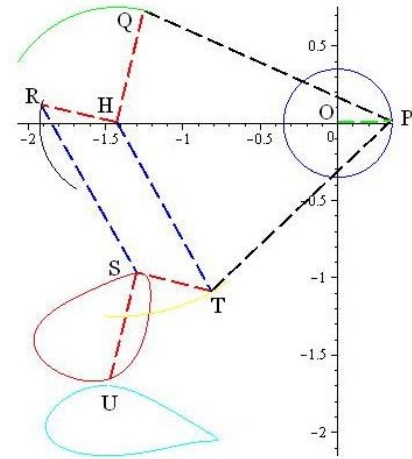


Figure 14: Trumm Leg with the Paths

## 2.6 Summary

We derived the parametric equations describing the position of each moving point on five different legs that can be used for at least two different transportation purposes. Using the properties of IV ODEs allowed us to do this. The PSM allowed us to generate piecewise polynomials describing the angle(s) of the motion of the important pivots. In the next section we will take advantage of this to describe the kinematics of the motion of each of the five legs.

We also point out the interesting fact that even though  $\theta$  is non-periodic and unbounded,  $\alpha$  and  $\beta$  are periodic and bounded ( $\beta$  in the Thelwell Leg and  $\alpha$  and  $\beta$  in the Trumm Leg). In fact, neither  $\alpha$  or  $\beta$  extend an entire circle. That is, they only trace out a portion of the circle. These two phenomena are seen in Figure 4. (The periodicity is not seen in Figures 12 and 13 because we only show the approximate solutions for one period.) Although, the denominators defining  $\alpha$  and  $\beta$  can be zero, the geometry of the legs do not allow this. The numerators of  $\alpha$  and  $\beta$ , however, are periodically equal to zero. It is also rather easy to see from the form of the differential equations for  $\alpha$  or  $\beta$  that  $\alpha'$  and  $\beta'$  are bounded. We present a phase portrait for  $\beta$  for the Thelwell Leg in Figure 15. Also notice that the sign of  $\theta'$  determines the direction the foot will move in.

Figure 15 shows the vector field for  $\beta$  of the Thelwell Leg. We show solutions for  $\beta_0 = -0.085$  (Section 2.1),  $\beta_0 = 1.5$  and  $\beta_0 = 3$  in yellow ( $\beta_0 = 3$  is an example of an impossible initial condition). The horizontal blue curve represents where  $\beta'$  does not exist. The vertical blue curves are where  $\beta' = 0$ .

This figure shows that  $\beta$  is periodic and that  $\beta'$  is bounded.

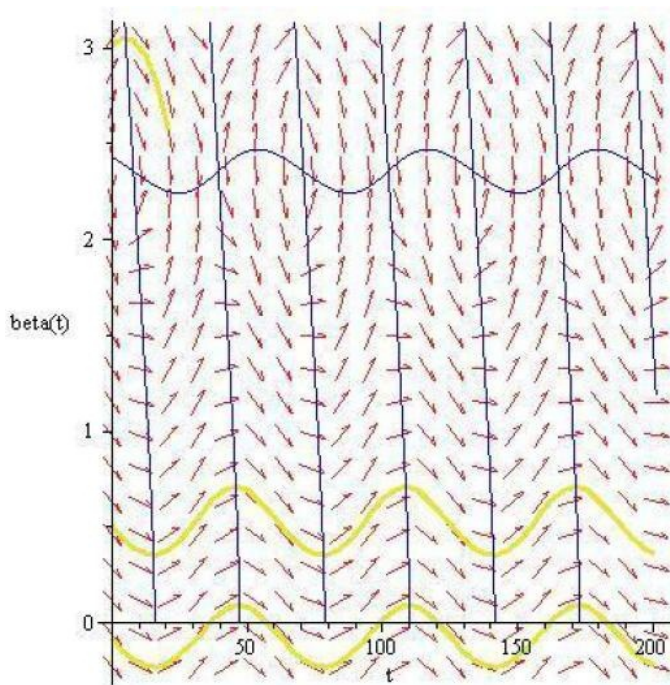


Figure 15: Phase Portrait for  $\beta$  of the Thelwell Leg

## 3 Kinetic Analysis

Since the PSM gives a polynomial in  $t$  for each interval  $(k-1)h \leq t \leq kh$ , where  $k$  is a natural number and  $h$  is a time step, and since both  $\alpha$  and  $\beta$  are approximated by polynomials for  $t \geq 0$ ,

we can differentiate the parametric equations for each moving point on any of the five legs. This allows us to obtain accurate approximations of the velocities and accelerations of these moving points by differentiating their corresponding parametric equations in  $t$ .

The engineers define the optimal leg for each of the five legs as the leg with the foot

- that touches the ground tangentially, implying that the velocity in the  $y$  direction is nearly zero at this time
- that travels with a large velocity in the direction parallel to the ground while on the ground
- that strikes the ground lightly, implying that the acceleration in the  $y$  direction is nearly zero at this time.

Sarani, Buehler, Koditschek point out that this is important for the legs in their six-legged RHEX robot [8]. However, they do not do a mathematical analysis, but mention that it is important to do one.

In this section we give the velocity and acceleration of the foot for each of the five legs presented in Section 2. We use

$$\vec{v} = (x', y') = (x'(t), y'(t))$$

for the velocity vector of a moving point and

$$\vec{a} = \vec{v}' = (v'_x, v'_y) = (x''(t), y''(t))$$

for the acceleration vector of a moving point. Therefore, the subscript  $x$  represents horizontal motion and the subscript  $y$  represents vertical motion.

The position, velocity and acceleration graphs of the foot for all five legs are displayed in Figures 16 - 30, where the graphs of the Thelwell foot are shown in Figure 16 - 18, Modified Thelwell foot - 19 through 21, Otto foot - 22 to 24, Thelwell/Otto foot - 25 through 27, and finally Trumm foot - Figures 28 - 30, respectively. Throughout this section the thinner line represents either position, velocity, or acceleration in the  $x$  direction (horizontal motion) and the thicker line in the  $y$  direction (vertical motion).

The graphs in Figures 16 - 18 show that the Thelwell Leg is not optimal for the engineer. That is, when the foot strikes the ground, it does not stay on the ground.

Analyzing the velocity graph of the Modified Thelwell foot (Figure 20), it is seen that from  $t \approx 37.5$  to  $t \approx 116.5$  the velocity in the  $y$  direction is approximately zero. This is desired because it implies that the leg is on the ground during that time period. However, the velocity in the  $x$  direction is not zero, it is negative, which means that the foot is moving backwards to bring the leg forward. The only time the velocity in the  $x$  direction is positive is when the leg is in the air, since the foot is moving clockwise. The extrema on the  $y$  velocity curve occur when the foot takes off the ground, which is desirable.

Analysis of the Otto foot graphs are similar, since they are just the inverted figures of the Modified Thelwell foot.

In Section 2.4 we talked about combining the Thelwell top part and the Otto bottom part together where point J is the foot of the system. Again, in the graphs of Thelwell/Otto foot the extrema on the  $y$  velocity curve detect the  $t$  when the foot leaves the ground and the zero velocity shows when it strikes the ground. Meanwhile, the velocity in the  $x$  direction moves the leg forward.

Finally, the shapes of the velocity and acceleration graphs of Trumm foot are similar to the Thelwell graphs. Thus, the analysis regarding the Thelwell Leg applies to the Trumm Leg.



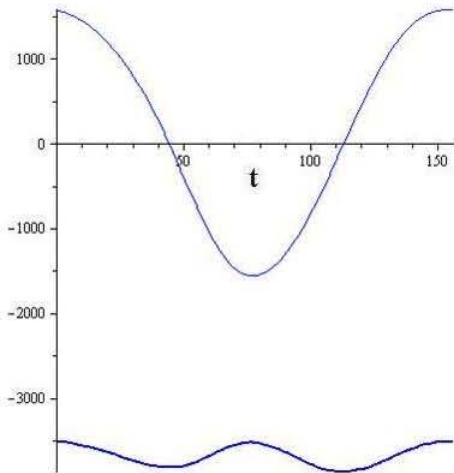


Figure 16: Position Graph of Thelwell Foot

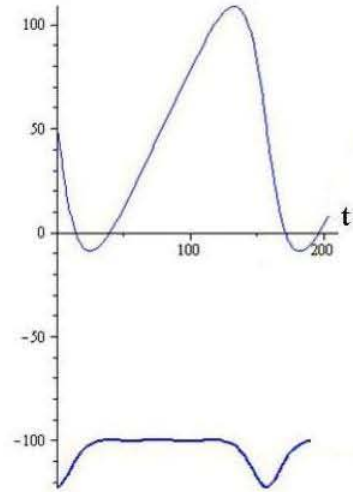


Figure 19: Position Graph of Modified Thelwell Foot

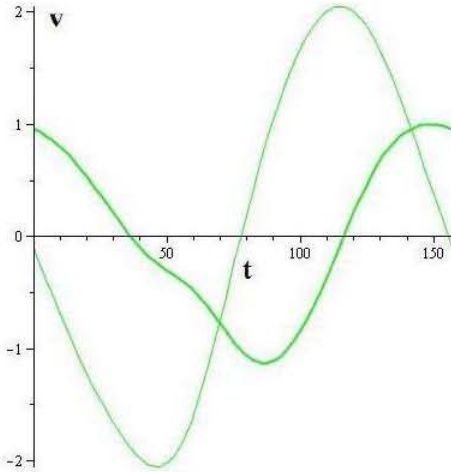


Figure 17: Velocity Graph of Thelwell Foot

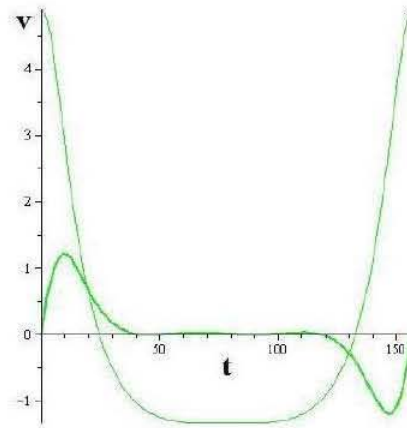


Figure 20: Velocity Graph of Modified Thelwell Foot

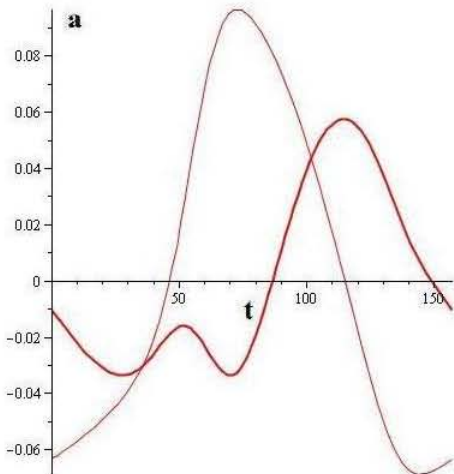


Figure 18: Acceleration Graph of Thelwell Foot

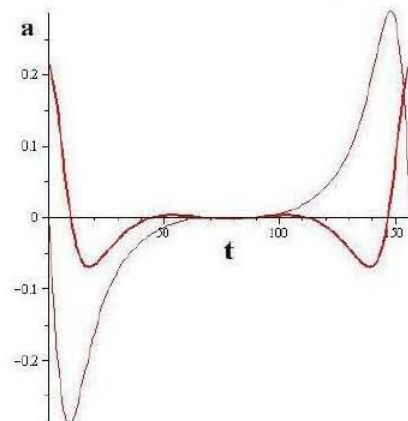


Figure 21: Acceleration Graph of Modified Thelwell Foot

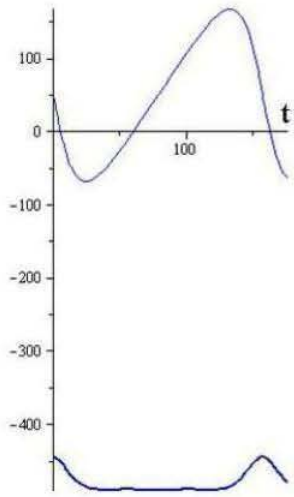


Figure 22: Position Graph of Otto Foot

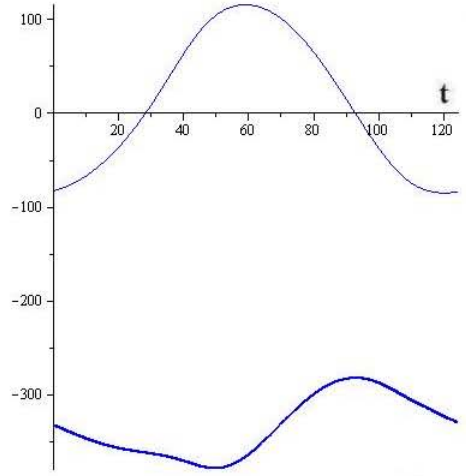


Figure 25: Position Graph of Thelwell/Otto Foot

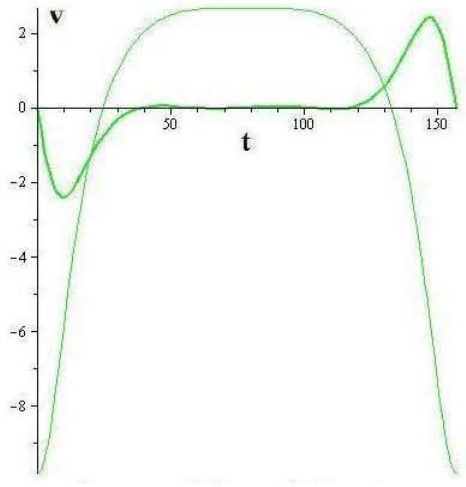


Figure 23: Velocity Graph of Otto Foot

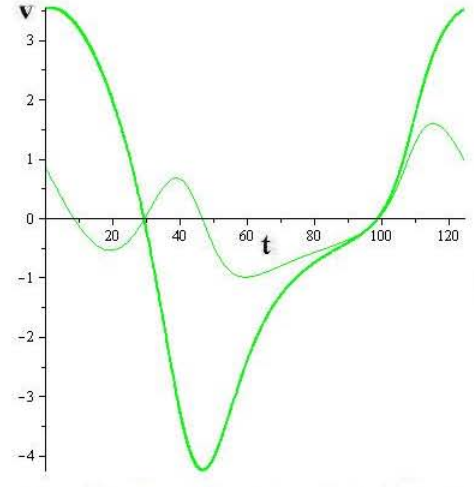


Figure 26: Velocity Graph of Thelwell/Otto Foot

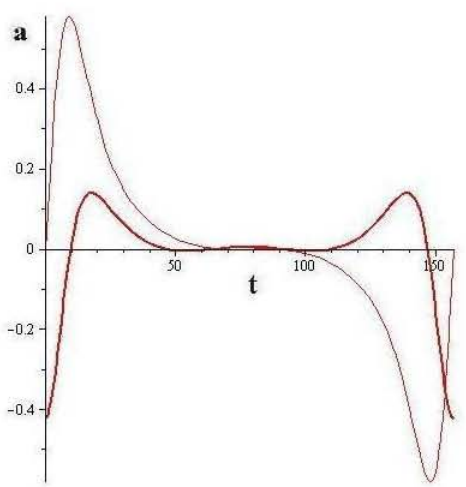


Figure 24: Acceleration Graph of Otto Foot

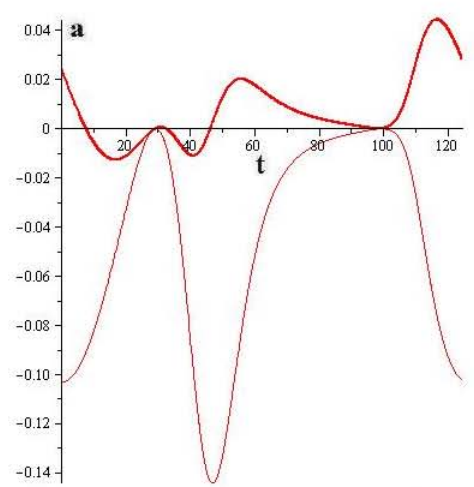


Figure 27: Acceleration Graph of Thelwell/Otto Foot

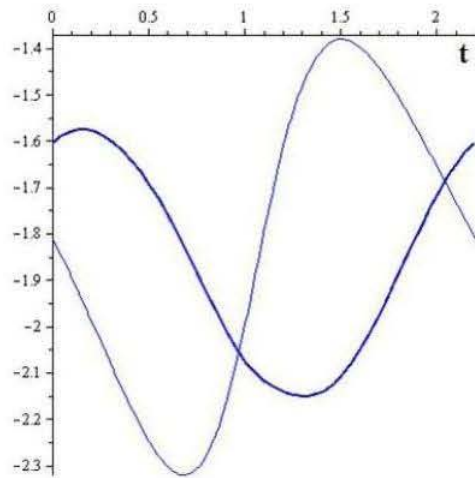


Figure 28: Position Graph of Trumm Foot

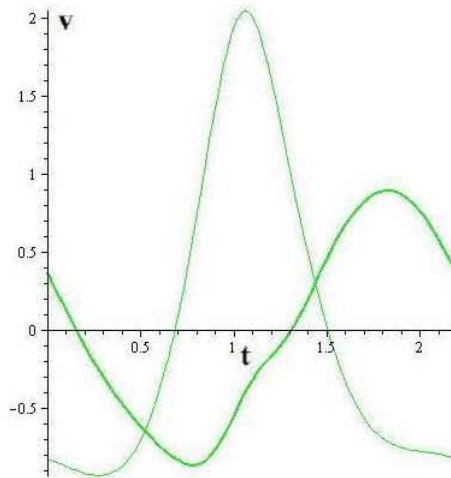


Figure 29: Velocity Graph of Trumm Foot

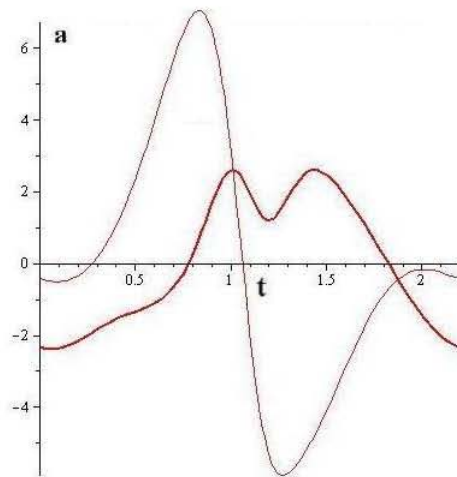


Figure 30: Acceleration Graph of Trumm Foot

## 4 Optimization

The definition of the optimal leg has not been standardized. However, we discussed many physical quantities that could be optimized to fit the engineer's optimal foot outlined in Section 3. For example, we looked at energy, power, force, and average power. Nevertheless, we believe that minimizing  $v_y^2 + a_y^2$  where  $v_y$  is the vertical component of velocity and  $a_y$  is the vertical component of acceleration of the foot corresponds to a soft (non-rigid) initial contact between the foot and the ground and in addition rapid movement of the foot while still on the ground, thus satisfying the optimal leg given in Section 3.<sup>7</sup> In this section we determine this optimal solution for the leg by minimizing

$$\mathcal{L} = \frac{1}{T} \int_0^T (v_y^2 + a_y^2) dt.$$

For the Modified Thelwell Leg we minimize  $\mathcal{L}$  by finding the coordinates of  $C = (u, v)$  for the foot (point R in Figure 7). That is,

$$\mathcal{L}(u, v) = \frac{1}{T} \int_0^T (v_{R_y}^2 + a_{R_y}^2) dt,$$

where

$$T = \frac{2\pi \cdot r_{OQ}}{vel}$$

with  $vel = 1$  for simplicity.  $v_R$  and  $a_R$  denote the velocity and acceleration of the foot, respectively.

We used Simpson's rule to do the integration in Maple and used Maple's Minimize command within the Optimization package to find the minimum of  $\mathcal{L}$ . We found the minimum of  $\mathcal{L}$  to occur at  $(50, 0)$  where Figure 31 depicts  $\mathcal{L}$  and displays the minimum. From this we conclude that the initial placement of the fixed point C was a good one because optimization gave us this as the answer (refer to Table 3 and Figure 7, Section 2.2).

Next, we optimized the Otto Leg, but now we used the fixed point G (knee) in Figure 8 to optimize the position of the fixed point H. Thus, the function  $\mathcal{L}$  is

$$\mathcal{L}(u, v) = \frac{1}{T} \int_0^T (v_{G_y}^2 + a_{G_y}^2) dt,$$

where the definition of T is the same as above and  $(u, v)$  will be the optimized coordinates of point H.  $v_G$  and  $a_G$  are the velocity and acceleration of point G, respectively.

From this  $\mathcal{L}$  we found the optimum H to be  $(8.5, -207.5)$  instead of its original coordinates  $(50, -230)$  as shown in Table 6, Section 2.3. Figure 32 displays the graph of  $\mathcal{L}$  and shows its minimum. The optimized Otto Leg and the paths are shown in Figure 33.

Notice that the path of G in the optimized Otto Leg is not smooth. Therefore, there will be a mechanical disadvantage, which means there will be engineering difficulties mostly, as we observed experimentally, due to large torque at this point. However, in Section 2.3 the path of G in Figure 8 is smoother. Therefore, strictly minimizing this quantity will not fully optimize the mechanical system of the leg. Certainly, because of the PSM we have many quantities that can be optimized. However, it is not computationally possible to optimize all of them.

---

<sup>7</sup>This measure was developed after discussions on power, energy and mechanical disadvantage with Dorn Peterson [5], a professor in the Department of Physics at JMU.

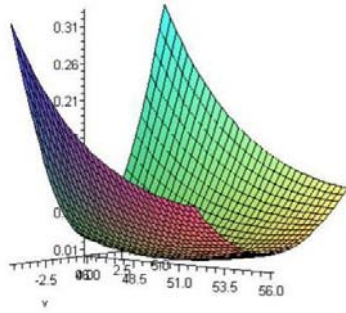


Figure 31: Optimization of Thelwell Modified Leg

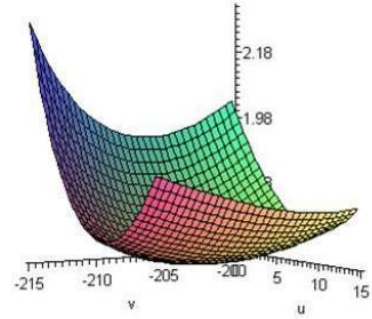


Figure 32: Optimization of Otto Leg

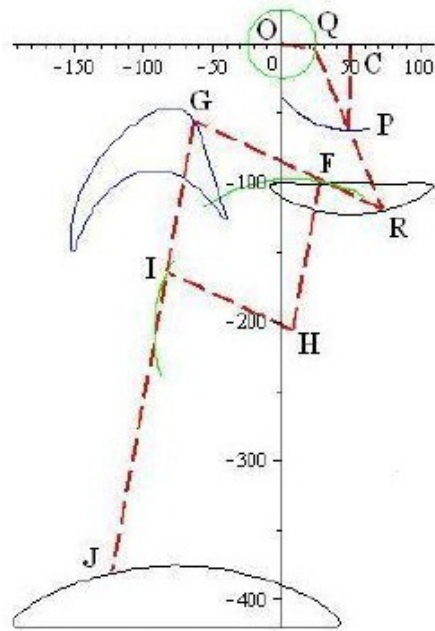


Figure 33: Optimized Otto Leg

## 5 Conclusion

We have demonstrated that it is possible to mathematically describe the motion of the foot for many types of legs for different transportation uses. The platform we have built allows us to mathematically analyze important elements of the motion of the leg. Finding the optimal leg, i.e. the best path traced out by the foot, is a computationally intensive problem. Therefore, techniques necessary to find quantities that can be optimized and give a quality designed leg need to be determined.

We did not address the issue of putting several legs of the same kind on one vehicle. Of course, this is also an important problem in efficient vehicular motion. The Department of Engineering at JMU is now working on this problem because of this study.

## References

- [1] W E Boyce and R C DiPrima. *Elementary Differential Equations*. John Wiley and Sons, Inc., 7 edition, 2000.
- [2] Delana. Unbelievable kinetic sculptures of theo jansen, 2008.
- [3] Florian Otto. Personal Communication, June - July 2009.
- [4] G. Edgar Parker and James S. Sochacki. Implementing the picard iteration. *Neural, Parallel Sci. Comput.*, 4:97–112, March 1996.
- [5] Dorn Peterson. Personal Communication, July 2009.
- [6] Carla Pinto and Martin Golubitsky. Central pattern generators for bipedal locomotion. *Journal of Mathematical Biology*, 53:474–489, 2006. 10.1007/s00285-006-0021-2.
- [7] Marc Raibert, Kevin Blankespoor, Gabriel Nelson, Rob Playter, and The BigDog Team. *Big-Dog, the Rough-Terrain Quadruped Robot*, pages 6–9. 2008.
- [8] Uluc Saranli, Martin Buehler, and D. E. Koditschek. Rhex: A simple and highly mobile hexapod robot. *International Journal of Robotics Research*, 20(7):616 – 631, July 2001.
- [9] Roger Thelwell. Personal Communication, June - July 2009.
- [10] Stefan Trumm. Personal Communication, June - July 2009.

## Acknowledgements

This work was funded by NSF grant DMS 0552577.